Dyes and Pigments 123 (2015) 39–43

Contents lists available at ScienceDirect

Dyes and Pigments

journal homepage: www.elsevier.com/locate/dyepig

Synthesis and spectroscopic properties of a FRET pair based on PPO and DBD dyes

Robert Wawrzinek, Pablo Wessig*

Institut für Chemie, Universität Potsdam, Karl-Liebknecht-Str. 24–25, D-14476 Potsdam, Germany

ARTICLE INFO

Article history:
Received 12 May 2015
Received in revised form
11 July 2015
Accepted 16 July 2015
Available online 28 July 2015

Keywords:
FRET
DBD
Pseudo Stokes shift
Microenvironmental probing

ABSTRACT

A new pair of Förster resonance energy transfer (FRET) performing fluorophores is introduced: An amine functionalized 2,5-diphenyloxazole (PPO) donor tethered via a flexible linker to a carboxylic acid functionalised ester-[1,3]-dioxolo[4.5-*f*][1,3]benzodioxole (ester DBD) acceptor. Synthesis and spectroscopic properties of this proof-of-concept molecule in acetonitrile are presented and compared to those of its independent chromophores. The system exhibits a Förster distance of 2.9 nm, high FRET efficiency of 0.88 and a pseudo Stokes shift of 190 nm.

1. Introduction

DBD dyes are a relatively new class of small molecules exhibiting large Stokes shifts, fluorescence in the VIS region and other interesting properties, such as high fluorescence lifetime (FLT) and in some cases extraordinary sensitivity of the latter to their microenvironment [1,2]. This behaviour has been successfully exploited in biological applications to show conformational changes in proteins and to develop an FLT based assay for acetylpolyamine amidohydrolases [3,4].

Such highly sensitive probes provide important information about their molecular surrounding and are powerful tools for understanding biological mechanisms. However, the most popular approach to investigate microenvironmental changes is to measure exchange of energy between two fluorophores via Förster resonance energy transfer (FRET) [5–7]. Here an energetically excited donor transfers its energy radiationless via dipole–dipole interaction to an acceptor molecule. Through this mechanism it is possible to observe acceptor emission (or donor emission quenching) despite irradiation in the wavelength region of donor absorption. Due to its strong distance dependency FRET systems are often called 'spectroscopic rulers' as they provide the opportunity to measure the distance between FRET pair molecules. This interaction is possible if donor and acceptor address certain parameters: the resonance frequency of the donor in the excited state needs to match the corresponding frequency of the acceptor in the ground state which is usually the case when the donor's emission spectrum overlaps with the acceptor's absorption spectrum. Also crucial for an effective FRET is the donor's fluorescence quantum yield and lifetime in absence of the acceptor, the relative alignment of the transition dipole moments of both chromophores, and of course the distance between them [8].

Herein we report on a new pair of FRET active chromophores showing a highly efficient energy transfer combined with a pseudo Stokes shift of 190 nm in acetonitrile. Fig. 1 shows the chemical structure of the independent donor and acceptor molecules as well as the FRET active proof-of-concept molecule **1**.

The motivation to design **1** was to find an appropriate donor for the ester-DBD fluorophore. The latter was chosen because it shows high fluorescence quantum yields not only in organic solvents but also in water [3]. As we will show 2,5-diphenyloxazole (PPO) turns out to be an ideal partner for the ester-DBD acceptor as it can be easily functionalised and matches with the spectroscopic requirements to function as a donor. Although its absorption maximum is around 300 nm, it has been shown that PPO can be excited with two-photon spectroscopy (hence pushing its theoretical absorption to 600 nm) making it interesting in

* Corresponding author.
E-mail address: wessig@uni-potsdam.de (P. Wessig).

http://dx.doi.org/10.1016/j.dyepig.2015.07.022
0143-7208/

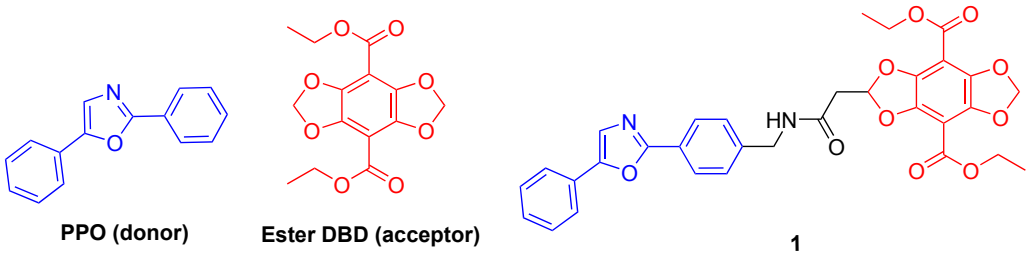

Fig. 1. Chemical structure of used chromophores and the target molecule **1**.

biological applications [9,10]. To the best of our knowledge this is the first time that PPO is used as a donor in an FRET system. Although this specific system is not soluble in water, the proof-of-concept, carried out in acetonitrile, is transferable to aqueous conditions because both chromophores show low solvatochromism and should behave in a similar manner.

2. Results and discussion

2.1. Synthesis

The synthetic route to target molecule **1** is depicted in Scheme 1. Commercially available BOC-protected *p*-aminomethyl benzoic

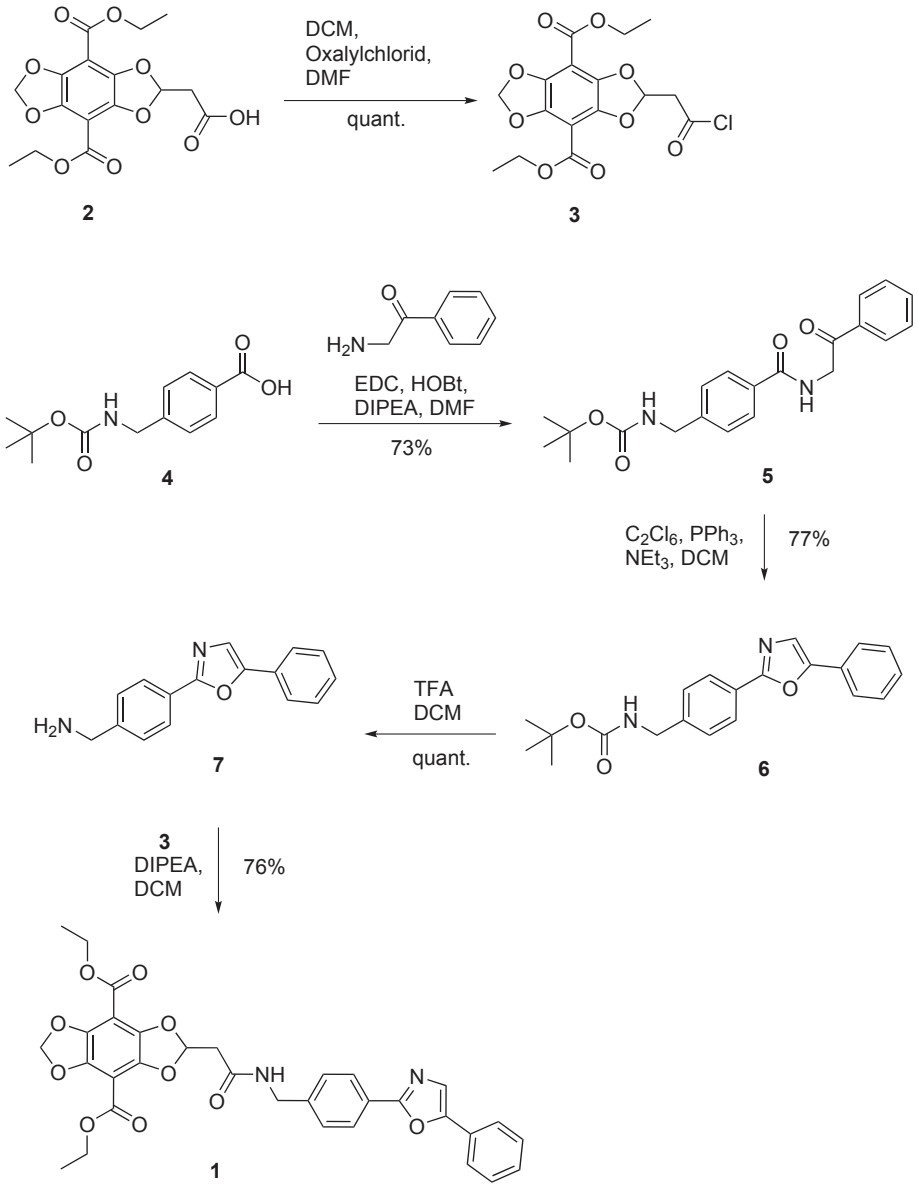

Scheme 1. Synthetic route to target molecule **1**.

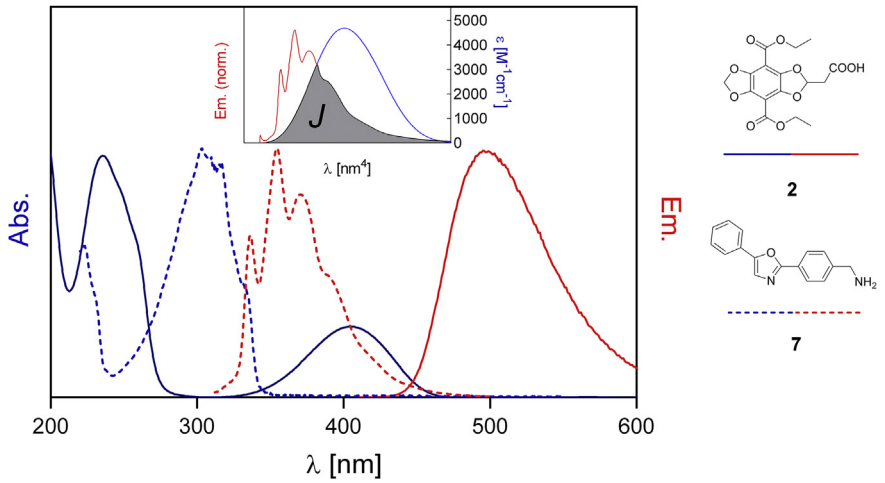

Fig. 2. Absorption and emission spectra of PPO **7** (dashed lines) and ester-DBD **2** (solid lines) in acetonitrile. The inset shows the overlap integral *J* used in Eq. (1).

acid **4** was coupled to 2-aminoacetophenone using 1-ethyl-3-(3-dimethylaminopropyl)carbodiimide (EDC) and *N*-hydroxybenzotriazole (HOBt) under classic peptide coupling conditions [11].

The following Appel cyclisation to oxazole **6** under mild conditions and subsequently deprotection gave amino PPO **7** in higher yields compared to previously reported approaches [12,13]. **7** was then coupled to the acid chloride **3** of ester-DBD **2** [3]. The resulting target molecule **1** contained the donor and acceptor fluorophores separated by a flexible non-conjugated amide linker.

2.2. Spectroscopic properties

As mentioned before the reason we selected PPO as a donor and the ester-DBD as an acceptor is their matching spectral overlap and the fact that both systems exhibit high fluorescence quantum yields (in acetonitrile 0.99 (**7**) and 0.56 (**2**), respectively). Fig. 2 shows the absorption and emission spectra of the independent chromophores. It is notable that the two broad absorption maxima of **2** ($\pi \rightarrow \pi^*$ around 240 nm and $n \rightarrow \pi^*$ around 400 nm) are baseline separated at the $\pi \rightarrow \pi^*$ absorption maximum of **7** (301 nm), which sits almost exactly in between. This ensures that donor excitation will not accidentally excite the acceptor.

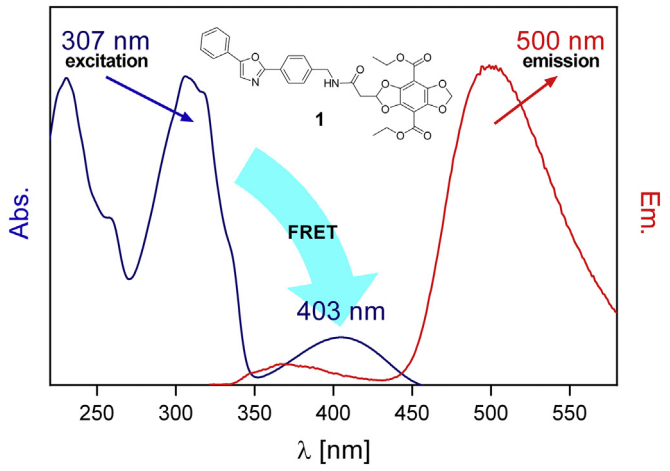

Fig. 3. Absorption (blue) and emission (red) spectra of **1** (excitation wavelength: 307 nm) in acetonitrile (For interpretation of the references to color in this figure legend, the reader is referred to the web version of this article.).

This becomes evident in Fig. 3 where absorption and emission spectra of target molecule **1** are presented. Due to the non-conjugated linker the absorption spectrum is almost the sum of the absorptions of the individual chromophores. Moreover, regardless which excitation wavelength was chosen, emission was almost exclusively detected at 500 nm, which indicated that nearly all energy absorbed by the PPO donor was transferred to the DBD acceptor. The small amount of detected donor emission (around 370 nm) arises when the orientation of its transition dipole moment is not matching with the acceptor's. This could be caused by a restricted conformational flexibility of the linker between the fluorophores and therefore weakening the FRET. To confirm our assumption that an FRET takes place we measured the excitation spectrum depicted in Fig. 4, which clearly shows the acceptor's strong emission when excited at the donor's absorption maximum around 300 nm.

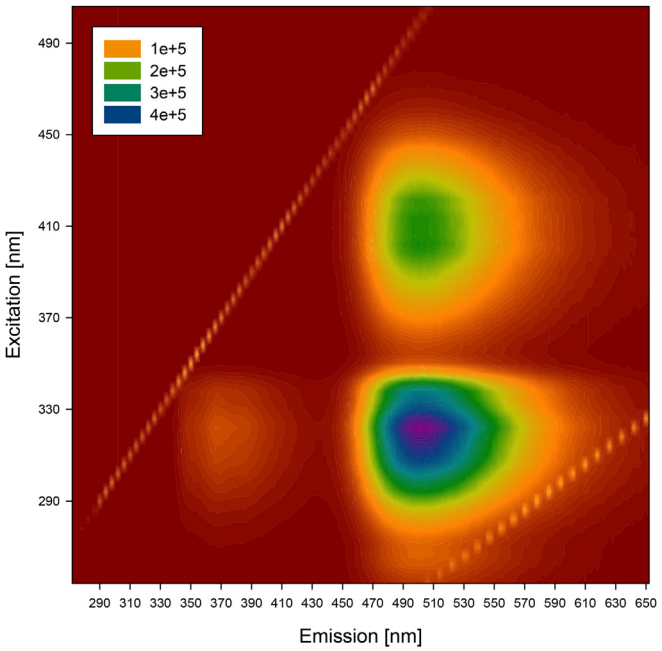

Fig. 4. Excitation spectrum of **1** in acetonitrile.

Table 1
Spectroscopic properties of **1**, **2**, **7** and calculated FRET parameters of **1**.

Compound	λ_{abs} [nm]	λ_{em} [nm]	Φ_F	τ_F [ns]	ε [M^{-1} cm^{-1}]	R_0 [nm]	E
1	307, 403	495	0.74[a] (0.62)	1.54[b] (15.40)	–	2.9	0.88
2 [3]	403	495	0.56	15.40	4680 (403 nm)		
7	307	378	0.99	1.66	35700 (301 nm)		

[a] Value includes donor and acceptor emissions. In brackets: only acceptor emission.
[b] Excitation at 254 nm, detection at 353 nm. In brackets: detection at 495 nm.

To further characterise the system we determined the fluorescence quantum yield at different excitation wavelengths and its fluorescence lifetime. The Förster distance R_0 (*e.g.* the distance between donor and acceptor in which the FRET efficiency is 0.5) was derived from the spectral overlap integral J using the normalised spectra of the donor's emission and the acceptor's molar extinction coefficient plotted against the fourth power of the wavelength (inset Fig. 2) and used in Eq. (1) [8].

$$R_0^6 = \frac{9 \cdot \Phi_D \cdot \kappa^2}{128 \cdot \pi^5 \cdot N_A \cdot n_D^4} \int_0^\infty F_D(\lambda)\varepsilon_A(\lambda)\lambda^4 d\lambda \quad (1)$$

Here κ^2 is the orientation factor (2/3), n_D the refractive index of the used solvent (1.344 for acetonitrile) and Φ_D the fluorescence quantum yield of the donor in absence of an acceptor (0.99). The integral term represents the mentioned spectral overlap J in which $F_D(\lambda)$ is the donor's normalised fluorescence intensity and $\varepsilon_A(\lambda)$ the acceptor's molar extinction coefficient. R_0 was determined to be 2.90 nm.

The fluorescence quantum yield (Φ_F) of **1** revealed a remarkable high value of 0.74 which, however, needed to be corrected as there was little donor emission detected. Measurements using excitation at 403 nm gave the fluorescence quantum yield Φ_A exclusively caused by the acceptor (0.62). This value was then subtracted from the initial measurement to obtain Φ_{DA}, the donor's quantum yield in presence of the acceptor (0.12).

Because this system shows no 'crosstalk' (the simultaneous excitation of donor and acceptor) and F_D (the donor's quantum yield in absence of an acceptor) is 0.99, we used Eq. 2 to calculate a FRET efficiency E of 0.88.

$$E = 1 - \frac{\Phi_{DA}}{\Phi_D} \quad (2)$$

We have chosen the fluorescence quantum yield to determine E rather than the often used fluorescence lifetime of the donor. The reason for that is the marginal influence of the acceptor on the already short lifetime of the donor (see Table 1), which causes larger errors due to a poor signal-noise ratio. Furthermore, it would be only legitimate to use lifetime measurements for a fixed distance between donor and acceptor and a monoexponential decay which is not complied by compound **1** due to its flexible linker.

At this point it is important to note that an efficiency of greater than 0.99 was expected because the distance between the fluorophores' centres could be maximal 1.3 nm (found by computational modelling). This means the in Eq. (1) used assumption of $\kappa^2 = 2/3$ for that particular molecule **1** is not correct [14]. However, it is legitimate to determine R_0 to generally describe a donor–acceptor system under the assumption of fully randomised orientation [15]. Furthermore, compound **1** falls into the category of FRET systems in which donor and acceptor are considered to be "too close" to each other ($r > 2$ nm) causing deviation from the ideal dipole approximation (IDA) [16]. As a consequence it is not valid for that particular system **1** to calculate parameters based on Eq. (1) such as the transition rate $k_T(r)$ (Eq. (3)).

$$k_T(r) = \frac{1}{\tau_D}\left(\frac{R_0}{r}\right)^6 \quad (3)$$

3. Conclusion

In this work we presented a new pair of FRET active fluorophores containing two small molecules; PPO as an UV absorbing donor and a green emitting ester-DBD dye acting as an acceptor. Using mild reaction conditions and peptide coupling techniques gave an easily accessible proof-of-concept molecule which than was spectroscopically investigated. Irradiated with light at the donor's excitation wavelength of 307 nm this molecule emitted acceptor fluorescence at 495 nm with a pseudo Stokes shift close to 190 nm and a fluorescence lifetime of 15 ns in acetonitrile. An FRET efficiency of 0.88 and a Förster distance of 2.90 nm were found. This new promising FRET pair could be a very useful addition to the DBD based tool box for microenvironmental probing. We are currently working on first applications and other FRET systems containing DBD dyes. Their large Stokes shifts, high fluorescence quantum yields and long fluorescence lifetimes provide huge advantages especially in FLT based microscopic and spectroscopic investigations.

Especially systems where a DBD moiety would function as FRET donor are of interest because the long FLT of DBD dyes would be transferred to the acceptor allowing for time gated temporal discrimination of background emission at a more red-shifted range of the visual spectrum.

4. Experimental

4.1. Spectroscopy

UV–vis measurements were performed with a JASCO V-630 spectrophotometer and analysed with Spectra Manager 2 (v 2.08.01). For all measurements square quartz cells (1 × 1 cm) were used.

Steady-state fluorescence spectra were measured with a Horiba Jobin Yvon Fluoromax 4 and analysed with FluorEssence (v 2.5.2.0). Fluorescence lifetime spectroscopy was performed on a Horiba Jobin Yvon Single Photon Counting Controller (TCSPC) Fluorohub with various LASER-diodes (NanoLED-254/372/447) used in combination with the mentioned spectrometer and the Datastation (v 2.5) software. To analyse the spectra DAS6 (v 6.4) was used. Fluorescence quantum yields were measured with a Hamamatsu Photonic Multi-Channel Analyzer C10027.

4.2. Syntheses

4.2.1. Diethyl 2-(2-oxo-2-((4-(5-phenyloxazole-2-yl)benzyl)amino) ethyl)benzo-[1,2-d:4,5-d′]bis([1,3]dioxol)4,8-dicarboxylate (**1**)

Acid chloride **3** (53 mg, 0.136 mmol) was dissolved in 10 mL dry dichloromethane and cooled down to 0 °C. Amine **7** (68 mg, 0.271 mmol) and *N*,*N*-diisopropylethylamine (23 μL, 0.136 mmol) were added and the mixture was stirred over night at room

temperature. After adding 50 mL dichloromethane the organic layer was separated and washed with saturated $NaHCO_3$ solution and brine. The separated organic layers were dried over $MgSO_4$, and the solvent evaporated in vacuo. The residue was purified using flash column chromatography (dichloromethane/methanol 25:1) to obtain 30 mg of compound **1** (50 μmol, 37%), and starting material **2** (25 mg, 67 μmol, 50%).

^{1}H NMR (δ/ppm, DMSO-d_6/pyridine-d_5, 300 MHz): 1.21 (t, $^3J = 7.11$, 6H, $-CH_3$); 3.19 (d, $^3J = 5.30$, 2H, $-CH_2$); 4.55 (d, $^3J = 5.90$, 2H, $-CH_2$); 4.60 (d, $^3J = 5.96$, 4H, $-CH_2$); 6.16 (s, 2H, $-CH_2$); 7.30–8.20 (10H, −CH). Mp: 239 °C. TLC: dichloromethane/methanol (100:4) $R_f = 0.31$. MS: (ESI) $m/z = 601.1814$ $[M + H]^+$, calc.: 601.1822. IR: 3274, 2923, 1723, 1638, 1551, 1496, 1453, 1416, 1294, 1174, 1081, 1023, 955, 759 cm^{-1}.

4.2.2. Compound **2**

Compound **2** was synthesised according to the literature [3].

4.2.3. Diethyl 2-(2-chloro-2-oxoethyl)benzo[1,2-d:4,5-d′]bis([1,3]dioxole)-4,8-dicarboxylate (**3**)

Compound **2** (50 mg, 0.137 mmol) was dissolved in 5 mL dry dichloromethane and oxalylchloride (82 μL, 0.95 mmol) as well as one drop dry DMF were added. After stirring for 4 h the solvents were carefully evaporated in vacuo (max. 50 mbar) to obtain acid chloride **3**, which was immediately used without any further purification.

4.2.4. tert-Butyl (4-((2-oxo-2-phenylethyl)carbamoyl)benzyl)carbamate (**5**)

Carboxylic acid **4** (1.2 g, 4.78 mmol) was dissolved in 40 mL dry DMF and 1-ethyl-3-(3-dimethylaminopropyl)carbodiimide·HCl (916 mg, 4.78 mmol), *N*,*N*-diisopropylethylamine (1 mL, 5.73 mmol) as well as *N*-hydroxybenzotriazole (645 mg, 4.78 mmol) were added. After 30 min additional 676 μL *N*,*N*-diisopropylethylamine (3.82 mmol) and subsequently 2-aminoacetophenone·HCl (682 mg, 4.78 mmol) were added and the mixture was stirred over night at room temperature. After adding 60 mL ethyl acetate and washing with 50 mL saturated $NaHCO_3$ the combined organic layers were dried over $MgSO_4$, the solvent evaporated in vacuo and the residue purified using flash column chromatography (hexane/ethyl acetate 2:1 to 1:1) to obtain 1.28 g of compound **5** (3.47 mmol, 73%) as a colourless solid.

^{1}H NMR (δ/ppm, $CDCl_3$, 300 MHz): 1.44 (s, 9H, $-CH_3$); 4.33 (s, 2H, $-CH_2$); 4.91 (d, $^3J = 4.01$, 2H, $-CH_2$); 7.30–8.08 (9H, −CH); 7.59 (t, $^3J = 7.57$, H, −NH). ^{13}C NMR (δ/ppm, $CDCl_3$, 75 MHz): 28.3 (3C); 44.2 (1C); 46.8 (2C); 79.6 (2C); 79.6 (1C); 127.4–128.9 (8C); 132.7 (2C); 134.3 (1C); 143.1 (1C); 155.9 (1C); 167.0 (1C); 194.3 (1C). Mp: 135–137 °C. TLC: hexane/ethyl acetate 1:1 $R_f = 0.51$. MS: (ESI) $m/z = 369.1804$ $[M + H]^+$, calc.: 369.1814. IR: 3335, 2977, 2922, 1693, 1648, 1534, 1503, 1450, 1392, 1365, 1251, 1225, 1168, 1002, 866, 751, 690 cm^{-1}.

4.2.5. tert-Butyl (4-(5-phenyloxoazole-2-yl)benzyl)carbamate (**6**)

2.14 g PPh_3 (8.11 mmol) was dissolved in 25 mL dry dichloromethane and cooled to −10 °C. Hexachloroethane (3.84 g, 16.21 mmol), NEt_3 (2.25 mL, 16.21 mmol) and amide **5** (905 mg, 2.46 mmol, dissolved in 30 ml dry dichloromethane) were added to the solution. After stirring for 30 min 10 mL dry dichloromethane was added and again stirred for 2 h at room temperature. After that period of time the mixture was washed with saturated NH_4Cl and subsequently saturated $NaHCO_3$ solution.

The separated organic layers were dried over $MgSO_4$, the solvent evaporated in vacuo and the residue purified using flash column chromatography (hexane/ethyl acetate 3:1 (+10% $CHCl_3$)) to obtain 660 mg of PPO derivate **6** (1.88 mmol, 77%) as a bright yellow solid.

^{1}H NMR (δ/ppm, $CDCl_3$, 300 MHz): 1.47 (s, 9H, $-CH_3$); 4.36 (s, 2H, $-CH_2$); 7.30–7.48 (6H, −CH); 7.65–8.10 (4H, −CH). ^{13}C NMR (δ/ppm, $CDCl_3$, 75 MHz): 28.4 (3C); 44.4 (1C); 79.7 (1C); 123.2 (1C); 124.18–128.9 (10C); 141.5 (1C); 151.2 (1C); 155.9 (1C); 160.9 (1C). Mp: 121 °C. TLC: hexane/ethyl acetate 3:1 $R_f = 0.2$. MS: (EI) $m/z = 350.1642$ $[M^+]$, calc.: 350.1630. IR: 3341, 2977, 2927, 1696, 1497, 1366, 1271, 1251, 1169, 1135, 953, 866, 829, 762, 689, 487 cm^{-1}.

4.2.6. (4-(5-Phenyloxazole-2-yl)phenyl)methanamine (**7**)

632 mg of compound **6** (1.8 mmol) was dissolved in 12 mL dry dichloromethane, 2 mL trifluoroacetic acid (TFA) was added and the mixture stirred for 2.5 h at room temperature. The solvents and remaining TFA were evaporated in vacuo to obtain 450 mg of amine **7** (1.8 mmol, quant.) which was immediately used without further purification [13].

Acknowledgements

We thank Kathlen Brennenstuhl for the fluorescence quantum yield measurements and Prof. Michael U. Kumke for inspiring discussions.

References

[1] Wessig P, Wawrzinek R, Möllnitz K, Feldbusch E, Schilde U. Tetrahedron Lett 2011;52:6192–5.
[2] Wawrzinek R, Wessig P, Möllnitz K, Nikolaus J, Schwarzer R, Müller P, et al. Bioorg Med Chem Lett 2012;22:5367–71.
[3] Wawrzinek R, Ziomkowska J, Heuveling J, Mertens M, Herrmann A, Scheider E, et al. Chem Eur J 2013;19:17349–57.
[4] Meyners C, Wawrzinek R, Krämer A, Hinz S, Wessig P, Meyer-Almes F-J. Anal Bioanal Chem 2014;20:4889–97.
[5] Miyawaki A. Annu Rev Biochem 2011;80:357–75.
[6] Clegg RM. Curr Opin Biotech 1995;6:103–10.
[7] Clegg RM. The history of FRET. In: Lakowicz JR, Geddes CD, editors. Reviews in fluorescence. Berlin: Springer; 2006.
[8] Lakowicz JR. Principles of fluorescence spectroscopy. New York: Springer; 2006.
[9] Luchowski R. Chem Phys Lett 2011;501:572–4.
[10] Silva DL, De Boni L, Correa DS, Costa SCS, Hidalgo AA, Zillio SC, et al. Opt Mater 2012;34:1013–8.
[11] El-Faham A, Albericio F. Chem Rev 2011;111:6557–602.
[12] Wipf P, Miller CP. J Org Chem 1993;58:3604–6.
[13] Meyer H-J, Wolff T. Chem Eur J 2000;6:2809–17.
[14] Loura LMS. Int J Mol Sci 2012;13:15252–70.
[15] van der Meer BW, van der Meer DM, Vogel SS. Optimizing the orientation factor Kappa-squared for more accurate FRET measurements. In: Medinitz I, Hildebrandt N, editors. FRET – Förster resonance energy transfer: from theory to applications. Weinheim: Wiley VCH; 2013.
[16] Munoz-Losa A, Curutchet C, Krueger BP, Hartsell LR, Mennucci B. Biophys J 2012;13:15252–70.